

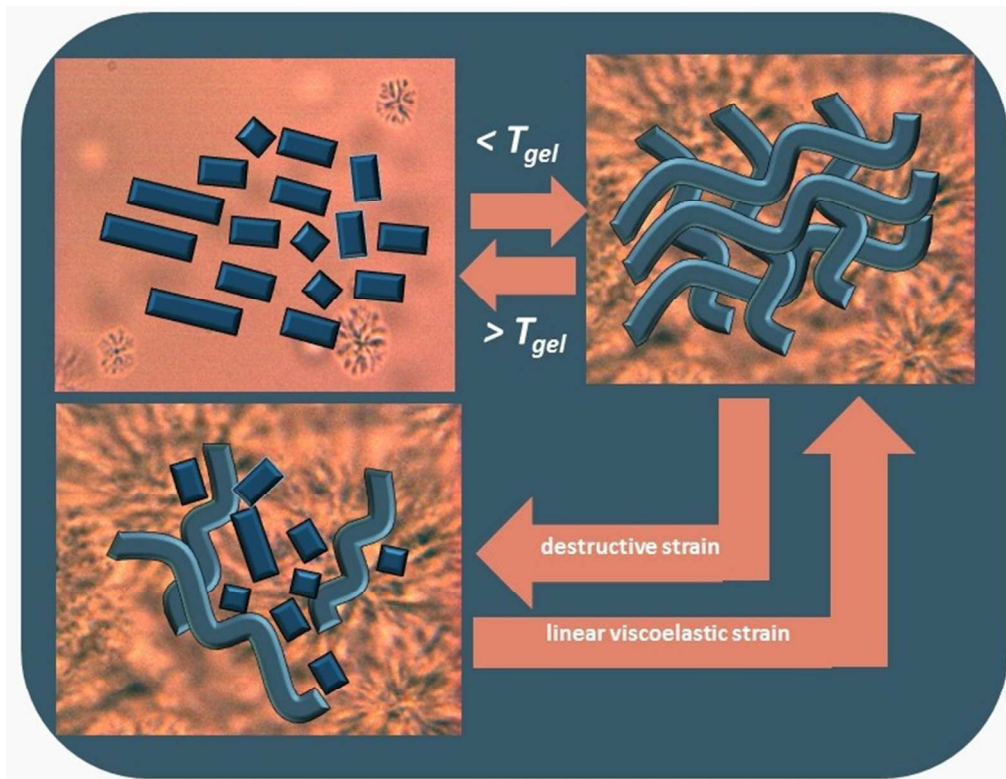


Structural bases for mechano-responsive properties in molecular gels of (*R*)-12-hydroxy-*N*-(ω -hydroxyalkyl)octadecanamides. Rates of formation and responses to destructive strain.

| | |
|-------------------------------|---|
| Journal: | <i>Soft Matter</i> |
| Manuscript ID: | SM-ART-02-2015-000353.R1 |
| Article Type: | Paper |
| Date Submitted by the Author: | 17-Apr-2015 |
| Complete List of Authors: | Weiss, Richard; Georgetown University, Department of Chemistry Mallia, V. Ajay; Georgetown University, Chemistry |
| | |

Table of contents graphic

The time and degree of mechano-response to destructive strain by molecular gels can be controlled by design.



Structural bases for mechano-responsive properties in molecular gels of (*R*)-12-hydroxy-*N*-(ω -hydroxyalkyl)octadecanamides. Rates of formation and responses to destructive strain.

V. Ajay Mallia^a and Richard G. Weiss^{a,b*}

^a Department of Chemistry and ^b Institute for Soft Matter Synthesis and Metrology, Georgetown University, Washington, DC 20057-1227, USA.

Abstract

The self-assembly and gelation behavior of a series of (*R*)-12-hydroxy-*N*-(ω -hydroxyalkyl)octadecanamides (**HS-*n*-OH**, where *n* = 2, 3, 4 and 5 is the length of the alkyl chain on nitrogen), as well as those of two ‘model’ compounds, (*N*-(3-hydroxypropyl)octadecanamide (**S-3-OH**) and (*R*)-12-hydroxy-*N*-propyloctadecanamide (**HS-3**), have been investigated in a wide range of liquids. A unique aspect of some of the **HS-*n*-OH** gels is the degree and velocity of their recovery of viscoelasticity after the cessation of destructive shear. The recovery times vary from less than one second to hundreds of seconds, depending on the length of the ω -hydroxyalkyl group on nitrogen. The data indicate that the modes and dynamics of aggregation of the gelator molecules from incubation of a sol phase below the gel melting temperature, as analyzed by Avrami and fractal equations, cannot be used to explain the degree and dynamics of the thixotropy: sol-to-gel transformations involve assembly of 0-dimensional objects (i.e., individual gelator molecules) into 1-dimensional fibrils and then into 3-dimensional networks; recovery after mechano-destruction of gels requires only 1-dimensional to 3-dimensional re-assembly or re-association of 3-dimensional spherulitic objects. A model to understand the extreme sensitivity of the thixotropy on the length of the ω -hydroxyalkyl group in the **HS-*n*-OH** (which is based upon detailed comparisons among the dynamic properties of the gels, the morphologies of the neat gelators, and the fibrillar networks of the gels) invokes the

importance of the cleavage and reformation of H-bonds between fibers at ‘junction zones’ or between spherulitic objects.

Introduction

A variety of supramolecular self-assembled materials are able to change their mechanical properties reversibly upon being perturbed by an external stimulus, such as temperature, electromagnetic radiation, electric field, pH or mechanical stress.¹ The reversibility is a consequence of structural reorganizations on the microscopic distance scale that are sensed macroscopically. In many cases, the source of the microscopic changes can be traced to the loss or gain of weak, intermolecular interactions, such as H-bonding, electrostatic forces, π - π stacking, and London dispersion forces.² Molecular gels, made with low molecular-mass organogelators (**LMOGs**) that organize into 3-dimensional (3D) fibrillar networks (**SAFINs**) that entrap macroscopically the liquid in which they reside,³⁻⁸ have become an important part of this subclass of self-assembled materials.^{9,10} Examples of molecular gels that consist of **LMOGs** with photo- or electric-field responsive or redox-sensitive functional groups are known.¹¹

However, examples of molecular gels with crystalline **SAFINs** that exhibit reversible mechano-responsive properties (i.e., thixotropic gels, materials that regain a large part of their viscoelasticity after cessation of destructive mechanical strain) are rare, and there are no *a priori* design criteria for new types of **LMOGs** that lead to such gels;¹² their discovery remains a matter of serendipity.¹³ Thixotropy has been defined as the “reversible reduction and recovery of elastic modulus, yield stress and viscosity isothermally upon the application and removal of a destructive shear strain.”¹⁴ Examples of thixotropic materials range from paints and foods, to biological materials such as actomyosin,¹⁵ and tooth enamel.¹⁶ Most molecular gels, especially those in which the **SAFINs** are crystalline, are only weakly thixotropic; such gels usually regain

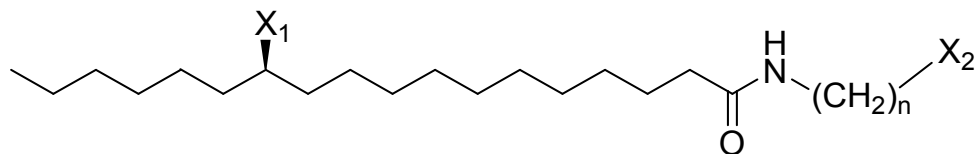
their full viscoelasticity only by heating the mixtures to their sol/solution states and re-cooling them to below the gel melting temperatures.

Many molecular gels with reversible thixotropic properties have organometallic **LMOGs**, so that their organization into a **SAFIN** (or its mechano-destruction) depends on the formation (or loss) of relatively weak metal-ligand bonds. An example is the thixotropic hydrogels with a Cu(II)-pyridyl terminated oligophenylenevinylene as the gelator.¹⁷ The **SAFINs** of many (but not all!) of these gels are non-crystalline¹⁸ or liquid-crystalline.¹⁹ Some examples that do not involve organometallic **LMOGs** are also known.¹² For example, toluene gels with *N*-(3-hydroxypropyl)dodecanamide as the **LMOG** have crystalline **SAFINs** and are known to exhibit very interesting thixotropic properties.²⁰ This and several other reports have attempted to explain the thixotropic behavior of molecular gels with crystalline **SAFINs**.²¹ In all these examples, restoration of the viscoelastic properties (and, therefore, reestablishment of the **SAFIN**) after mechanical disruption requires minutes to hours.

Earlier, we reported that molecular gels of 2 wt % (*R*)-12-hydroxyoctadecanamide in silicone oil are able to recover >90 % of their original viscoelasticity within 10 s after the cessation of destructive strain.²² Silicone oil gels of the corresponding secondary amides, (*R*)-12-hydroxy-*N*-alkyloctadecanamides, recovered only about one-half of their initial storage modulus (G') values after cessation of destructive strain. Within the class of gels consisting of one liquid and different derivatives of (*R*)-12-hydroxystearic acid (**HSA**) as the **LMOGs**, the degree of thixotropic recovery correlates qualitatively with the potential strength of hydrogen-bonding interactions among hydroxyl groups of the assembling molecules.²²

A somewhat related observation is that 'lubrication' by hydroxyl groups can induce liquid crystallinity in phosphonium halides.²³ For example, addition of 1 molar equivalent of

methanol to several solid methyl-tri-*n*-alkylphosphonium salts or introduction of an ω -hydroxyl group to a short alkyl group of a phosphonium salt with 3 long alkyl chains induces the formation of smectic liquid-crystalline phases. On those bases, we hypothesized that hydroxyl groups added to the terminal carbon atoms of the alkyl groups of the (*R*)-12-hydroxy-*N*-alkyloctadecanamides may augment the degree of thixotropy of their gels via a related form of ‘lubrication’ within their **SAFINs**. To test this hypothesis experimentally, we have investigated systematically the relationship between the molecular and **SAFIN** structures of a homologous series of (*R*)-12-hydroxy-*N*-(ω -hydroxyalkyl)octadecanamides (**HS-n-OH**) and the mechano-responsive properties of their gels (i.e., the eventual degree and kinetics of viscoelastic recovery after cessation of destructive strain). The results are compared with those from molecular gels containing an **LMOG** that lacks an ω -hydroxyl group on its *N*-alkyl chain ((*R*)-12-hydroxy-*N*-propyloctadecanamide, **HS-3**) and one that lacks a hydroxyl group at C12 of an octadecanamide (*N*-(3-hydroxypropyl)octadecanamide, **S-3-OH**). **S-3-OH** is a homologue of the previously reported thixotropic gelator, *N*-(3-hydroxypropyl)dodecanamide.²⁰ Thixotropic recovery of the **HS-n-OH**, **HS-3** and **S-3-OH**-based molecular gels can be ‘instantaneous’ (i.e., within the temporal limits of the instrumentation) or protracted, and virtually complete or nearly nil. These very different compartments have been interpreted on the basis of a model for intermolecular interactions within the **SAFIN** structures.



HS-n-OH: n = 2, 3, 4 and 5, X₁ = X₂ = OH

S-3-OH: n = 3, X₁ = H, X₂ = OH

HS-3: n = 3, X₁ = OH, X₂ = H

Experimental

Most of the information concerning instrumentation, procedures, and materials is included in Supporting Information;²² tables and figures from it are designated with an ‘S’ preceding the number. Procedures specific to this project are below.

Gels were prepared by placing weighed amounts of a liquid and gelator into a glass tube (5 mm, i.d.) that was then flame-sealed. The mixture was heated in a water bath until a solution/sol was obtained and then placed directly into an ice-water bath for 10 min. Slow-cooled gels were prepared using the protocol above except that the hot solutions/sols were kept in the water bath while they returned slowly to room temperature. All gel samples discussed here were prepared by the fast-cooling protocol unless indicated otherwise.

The critical gelator concentrations (*CGCs*) at room temperature (~25 °C) were determined from the samples with the lowest **LMOG** concentrations (prepared by the fast-cooling protocol) that did not flow perceptibly over a period of ~30 s when the ca. 5 mm (i.d.) tubes in which they were placed were inverted.²⁴ *CGCs* of samples in isostearyl alcohol, prepared by the fast-cooling protocol and kept at 25 °C for about ~60 h gels were determined by

rheological measurements at 25 °C; the criterion employed was based on the values of the storage (G') and loss (G'') moduli in the linear viscoelastic region (*vide infra*).

Gel melting temperatures (T_{gel}) were determined by the ‘falling drop method’;²⁴ the sealed glass tubes were inverted and placed in a water bath which was heated at ca. 1.5 °C/min; the temperature ranges over which the gels fell under the influence of gravity are reported. Gel melting temperatures determined by differential scanning calorimetry (DSC) are indicated as $T_{gel-DSC}$.

Atomic force microscopy (AFM) imaging was accomplished on a Bruker Bio Scope Catalyst microscope with peak force tapping using a Scan Asyst-Air probe ($k \sim 0.4$ N/m and tip radius < 10 nm) or NTEGRA Prima scanning probe microscope (NT-MDT) mounted on an inverted Nikon Eclipse Ti-S fluorescence microscope with peak force tapping using a probe (NSG 10, $k \sim 3.7$ - 37.6 N/m, tip radius, ~ 10 nm). The gel samples were prepared on glass micro slides (Corning 75 x 25 x 1 mm) using the fast-cooling protocol. Images were analyzed using Research Nanoscope 8.15 or Image Analysis 3.50.2090 NTMDT software.

General procedure for preparation of (R)-12-hydroxy-N-(ω -hydroxyalkyl)octadecanamides.²² Under a dry atmosphere, a solution of (R)-12-hydroxystearic acid (1.0 g, 3.3 mmol) and triethylamine (0.3 g, 3.3 mmol) in dry THF (25 mL) was added slowly to a vigorously stirred solution of ethyl chloroformate (1.80 g, 16.6 mmol) in dry THF (50 mL) while maintaining the temperature at 0 °C. The mixture was stirred for an additional 20 min at 0 °C. An ω -aminoalkan-1-ol (12 mmol) in 10 mL dry THF was added to the solution at 0 °C, and the reaction mixture was kept at room temperature for 10 h in a dry atmosphere. The solvent was removed by distillation at room temperature, and the residue was dissolved in ethyl acetate (50 mL), washed successively with 3N HCl (3X15 mL), aqueous 1M Na₂CO₃ (3X15

mL), and water (50 mL). The organic layer was dried over sodium sulfate and the residue, after evaporation, was recrystallized from ethyl acetate.

(R)-12-Hydroxy-*N*-(2-hydroxyethyl)octadecanamide (**HS-2-OH**). 85 % yield; mp 111.7-112.0 °C; IR (neat, cm^{-1}): 3304, 2910, 2820, 1640, 1549, 1466. $^1\text{H-NMR}$ (CDCl_3 , 300 (MHz): δ 0.91 (m 3H, CH_3) 1.2-1.6 (m, 28H, $-\text{CH}_2$), 2.17 (t, 2H, $-\underline{\text{CH}_2}-\text{CO}-$), 3.42 (m, 2H, $-\underline{\text{CH}}-\text{NH}$), 3.59 (m, 1H, $-\underline{\text{CH}}-\text{OH}$), 3.8 (t, $-\underline{\text{CH}_2}-\text{OH}$) 5.85 (br, 1H, $-\text{NH}-$). Elemental analysis calcd for $\text{C}_{20}\text{H}_{41}\text{NO}_3$: C 69.92, H 12.03, N 4.08, O 13.97; found C 69.90, H 12.07, N 4.09.

(R)-12-Hydroxy-*N*-(2-hydroxypropyl)octadecanamide (**HS-3-OH**). 75 % yield; mp 108.6-109.0 °C; IR (neat, cm^{-1}): 3300, 2910, 2824, 1643, 1549, 1466. $^1\text{H-NMR}$ (CDCl_3 , 300 (MHz): δ 0.91 (m 3H, CH_3) 1.2-1.6 (m, 28H, $-\text{CH}_2$), 1.7 (m, 2H), 2.17 (t, 2H, $-\underline{\text{CH}_2}-\text{CO}-$), 3.42 (m, 2H, $-\underline{\text{CH}}-\text{NH}$), 3.59 (m, 1H, $-\underline{\text{CH}}-\text{OH}$), 3.8 (t, $-\underline{\text{CH}_2}-\text{OH}$) 5.85 (br, 1H, $-\text{NH}-$). Elemental analysis calcd for $\text{C}_{21}\text{H}_{43}\text{NO}_3$: C 70.54, H 12.12, N 3.92, O 13.42; found C 70.51, H 12.11, N 3.94.

(R)-12-Hydroxy-*N*-(2-hydroxybutyl)octadecanamide (**HS-4-OH**). 45 % yield; mp 108.1-108.4 °C; IR (neat, cm^{-1}): 3302, 2910, 2820, 1641, 1549, 1466. $^1\text{H-NMR}$ (CDCl_3 , 300 (MHz): δ 0.90 (m 3H, CH_3) 1.2-1.6 (m, 32H, $-\text{CH}_2$), 2.1 (t, 2H, $-\underline{\text{CH}_2}-\text{CO}-$), 3.4 (m, 2H, $-\underline{\text{CH}}-\text{NH}$), 3.6 (m, 1H, $-\underline{\text{CH}}-\text{OH}$), 3.8 (t, $-\underline{\text{CH}_2}-\text{OH}$) 5.85 (br, 1H, $-\text{NH}-$). Elemental analysis calcd for $\text{C}_{22}\text{H}_{45}\text{NO}_3$: C 71.11, H 12.21, N 3.77, O 12.92; found C 71.18, H 12.14, N 3.84.

(R)-12-Hydroxy-*N*-(2-hydroxypentyl)octadecanamide (**HS-5-OH**). 65 % yield; mp 103.1- 103.5 °C; IR (neat, cm^{-1}): 3302, 2910, 2824, 1643, 1549, 1466. $^1\text{H-NMR}$ (CDCl_3 , 300 (MHz): δ 0.91 (m 3H, CH_3) 1.2-1.6 (m, 34 H, $-\text{CH}_2$), 2.2 (t, 2H, $-\underline{\text{CH}_2}-\text{CO}-$), 3.4 (m, 2H, $-\underline{\text{CH}}-\text{NH}$), 3.6 (m, 1H, $-\underline{\text{CH}}-\text{OH}$), 3.7 (t, $-\underline{\text{CH}_2}-\text{OH}$) 5.8 (br, 1H, $-\text{NH}-$). Elemental analysis calcd for $\text{C}_{23}\text{H}_{47}\text{NO}_3$: C 71.64, H 12.28, N 3.63, O 12.45; found C 71.68, H 12.24, N 3.69.

Results and Discussion

Self-assembly and gelation properties of HS-3, S3-OH and the HS-n-OH homologues.

SAFIN structures of organogels with amide derivatives of HSA as the LMOGs have been studied extensively.²² Those results indicate that the efficiency of gelation by HSA derivatives depends on the number, position, and type of H-bonding functional groups along the long alkyl chain.²² Here, the gelating properties of the HS-n-OH are investigated to elucidate the relationship between the molecular structures and the properties of the SAFINs in their gels, especially as they pertain to the induction of thixotropy. In addition, the gelating properties of two LMOGs structurally-related to HS-3-OH, one lacking an ω -hydroxyl group on the *N*-alkyl chain (i.e., HS-3) and the other lacking the hydroxyl group at C12 (i.e., S-3-OH), are included. A survey of the gelating abilities of the HS-n-OH, S-3-OH and HS-3 LMOGs in a wide range of liquids is summarized in Table 1.

Table 1. Appearances,^a T_{gel} or neat LMOG melting temperatures ($^{\circ}\text{C}$, in parentheses), and CGCs [wt %, in brackets] of gels containing 2 wt % HS-n-OH, S-3-OH or HS-3²² in various liquids.

| Liquid\gelator | HS-2-OH (111.7-112.0) | HS-3-OH (108.6-109.0) | HS-4-OH (108.1-108.4) | HS-5-OH (103.1-103.5) | S-3-OH (98.1-98.4) | HS-3 (107.1-107.5) |
|--------------------|--------------------------|--------------------------|--------------------------|--------------------------|-----------------------|-----------------------|
| Silicone oil | OG (107-108) [0.2] | OG (102-103) [0.08] | OG (85-86) [0.3] | TG (83-84) [0.3] | OG (80-81) [0.9] | OG (86-87) [0.3] |
| Water | P | P | P | P | OG (76-80) [1.3-2.0] | I |
| Acetonitrile | OG (67-70) [0.2] | OG (66-67) [0.2] | OG (64) [0.5] | OG(64-65) [0.5] | P | OG (62) [0.5] |
| Methanol | Soln | Soln | Soln | Soln | P | Soln |
| 1-Octanol | P | P | P | P | P | Soln |
| Isostearyl alcohol | OG (58-60) [0.8-1] | OG (57-60) [0.8-1] | OG (56-57) [0.6-0.7] | OG (50-55) [0.7-0.8] | OG (40-43) [1.2-2.0] | OG (52-54) [0.5-0.6] |
| Toluene | CG (82-83) [0.2] | CG (78-79), [0.2] | CG (66-67) [0.6] | CG (69-70) [0.5] | P | OG (55-58) [0.3] |
| CCl ₄ | OG (52-53) [0.3] | OG (48-49) [0.3] | OG (43) [0.4] | OG (44-45) [0.5] | P | OG (58-60) [0.3] |
| <i>n</i> -Hexane | I | I | I | I | I | OG (74-75) [1.5-2] |

^a OG-opaque gel, TG- translucent gel, P-precipitate, I-insoluble, Soln-solution

Based on the very low *CGC* values of their gels in silicone oil, acetonitrile, CCl_4 , and toluene (< 0.5 wt %), as well as in isostearyl alcohol (≤ 1.0 wt %), the **HS-n-OH** are exceedingly effective gelators. A clear silicone oil gel was formed at room temperature at as low as 0.08 wt % of **HS-3-OH**. As a consequence of the lack of an OH group on the octadecanoyl chain of **S-3-OH** and, thus, weaker overall hydrogen-bonding interactions, the *CGC* values of its silicone oil and isostearyl alcohol gels are slightly higher than those of the **HS-n-OH**. Although **S-3-OH** precipitated from toluene solutions/sols, only 1.1 wt % of its homologue, *N*-(3-hydroxypropyl)dodecanamide, is reported to form a gel.²⁰ We conjecture that increasing the alkanoyl chain length from 12 to 18 carbon atoms (in **S-3-OH**) increases London dispersive interactions in its aggregates so that the balance between solubilization in a liquid and precipitation from it (without **SAFIN** formation) is tilted in favor of precipitation. In that regard, the *CGC* value in isostearyl alcohol of **HS-3**, lacking a ω -hydroxyl group on the propyl chain, was the smallest of any of the investigated **LMOGs**.

As shown in Table 1, 2 wt % of the **HS-n-OH** formed precipitates in water, but solutions/sols in methanol. However, 2 wt % of **HS-2-OH** in 1/1 (wt/wt) methanol/water forms an opaque gel and **S-3-OH** forms hydrogels²⁵ as well as organogels in silicone oil and isostearyl alcohol. It was not possible to measure the *CGCs* of the gels in isostearyl alcohol using the inverted tube method: although they are very weak and flowed slowly when inverted, they are true gels according to rheological measurements (*vide infra*).

Structural and thermodynamic studies of HS-n-OH as neat solids and in SAFINs.
Although attempts to produce single crystals of the **HS-n-OH** suitable for structural analyses were unsuccessful, powder X-ray diffraction (XRD) peaks of the neat solids, crystallized from ethyl acetate, could be indexed satisfactorily to orthorhombic packing arrangements (Figures S1-

S4). Figure 1 shows a possible 'head-to-tail' packing arrangement of **HS-2-OH** based on reported XRD crystal data for the structurally similar methyl ester of **HSA**.²⁶ The calculated extended length of a molecule of **HS-2-OH** is 27.2 Å,²⁷ and the head-to-head distance in Figure 1, 54.3 Å, is in excellent agreement with the Bragg distance corresponding to the lowest reflection, 54.6 Å, in the neat powder of **HS-2-OH** (Table S1; *vide infra*). In a packing arrangement like that shown in Figure 1, intermolecular H-bonding interactions of two C12 hydroxyl groups and of two amide groups on adjacent molecules may help to stabilize the crystalline lattice. The ω -hydroxyl group-amide interactions, also apparent in Figure 1, may be an important contributor to the thixotropic properties found in the **HS-n-OH** gels (*vide infra*). The calculated length of another potential head-to-head dimer packing arrangement, analogous to the one found in *N*-(2-hydroxyethyl)octadecanamide²⁸ (Figure S5), is inconsistent with the XRD data. Although the morphs in the solid and gel are different for most of the **HS-n-OH** homologues, all except **HS-5-OH** seem to be in extended conformations as dimers and in the *general* shape shown in the Figure 1. However, H-bonding and other aspects of the intermolecular interactions must differ in subtle ways.

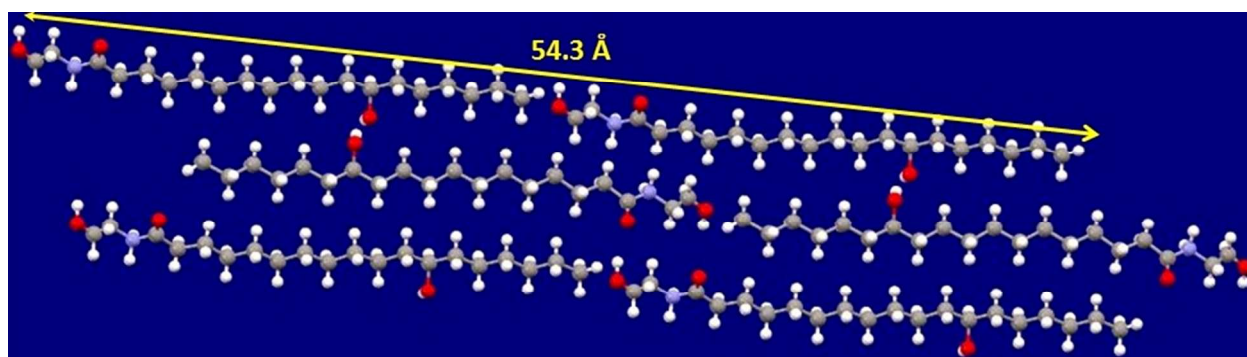


Figure 1. A possible packing arrangement of **HS-2-OH** molecules,²⁹ analogous to the single crystal packing arrangement reported for the methyl ester of **HSA**.

Table S1 summarizes the layer distances and refined cell parameters obtained from the XRD diffractograms of the neat solids. To understand the morphologies and packing

arrangements of the **SAFINs**, the data in Table S1 have been compared with those from diffractograms of the **HS-n-OH** in isostearyl alcohol gels. The diffraction peaks of the gels were located by subtracting empirically the “amorphous” scatter of isostearyl alcohol from the total gel diffractograms.³⁰ The same morph is present in the **SAFINs** of the gels and in the neat powders if the peaks in their diffractograms are found at the same values of 2θ . This appears to be the case for neat **HS-2-OH** and its isostearyl alcohol gel (Figure 2A), but not for the other **HS-n-OH** (Figure 2), and even the solvent-subtracted X-ray diffractogram of a 5 wt % **HS-2-OH** in toluene gel and that of neat **HS-2-OH** show different diffraction peaks (Figure S6A). In fact, many **LMOGs** are known to be polymorphic,³¹ and that is the case for the **SAFINs** of **HS-3-OH** as well (Figure S6).

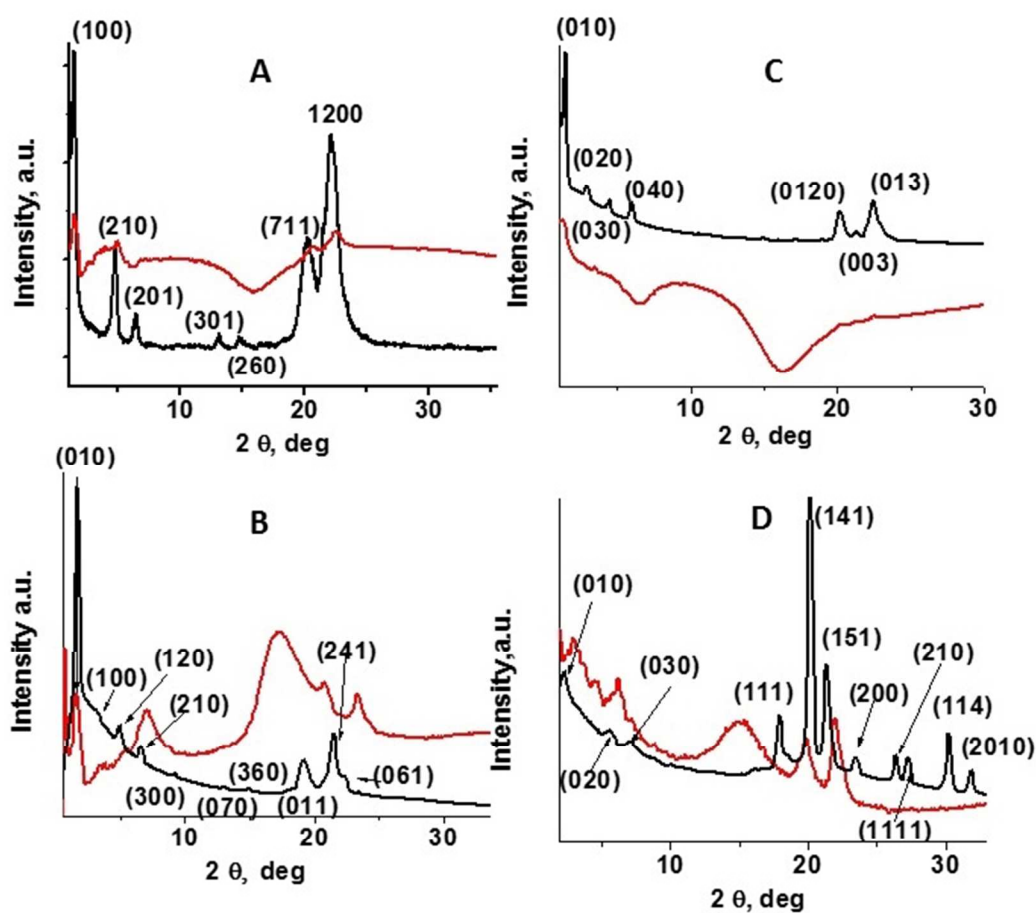


Figure 2. Vertically offset XRD patterns at 22 °C of neat **HS-n-OH** (black; crystallized from ethyl acetate) and their isostearyl alcohol gels (red) after empirical subtraction of the liquid component: (A) 4.8 wt % **HS-2-OH** gel; (B) 5.1 wt % **HS-3-OH** gel; (C) 5.0 wt % **HS-4-OH** gel; (D) 5.3 wt % **HS-5-OH** gel.

Radially averaged, 2-dimensional small-angle neutron scattering (SANS) scattering curves of a 2 wt % **HS-2-OH** in toluene- d_8 gel (Figure 3) were fitted well to a model for large objects with sharp interfaces; the scattering profile exhibits a power law decay of slope Q^{-4} .³² Analyses are based on the assumption that scattering is due mainly to the form-factor contribution of aggregated objects at the low **LMOG** concentrations employed.³² In addition, there is a broad Bragg reflection peak at $Q = 1.2 \text{ \AA}^{-1}$ that corresponds to a distance = 52.0 Å. This distance is in excellent agreement with the aforementioned bilayer packing arrangement in the neat powder and toluene gel of **HS-2-OH** (Table S1).

The fibrous structure of the **SAFINs** is evident in the polarized optical micrographs (POM) images of the corresponding fast- and slow-cooled gels in toluene (Figures S8 and S9). The entire scattering profile can be fitted satisfactorily to a theoretical curve for flexible cylinders with poly-radii: radius 28 Å. The calculated contour length, $1.7 \times 10^7 \text{ \AA}$, is an approximation, and neither the radius nor the Kuhn length depends acutely on its value.³³

To determine whether any change in morphology occurred as a result of the gel preparation protocol, 2 wt % **HS-2-OH** in silicone oil gels were prepared by fast- and slow-cooling protocols. Despite the differences between the sizes of the fibrillar objects in the **SAFINs** of the two gels (the slow-cooled gel having the larger objects as a result of the smaller driving force for phase separation from its sol³⁴ (Figures S10 and S11)), their T_{gel} values were the same within experimental error.

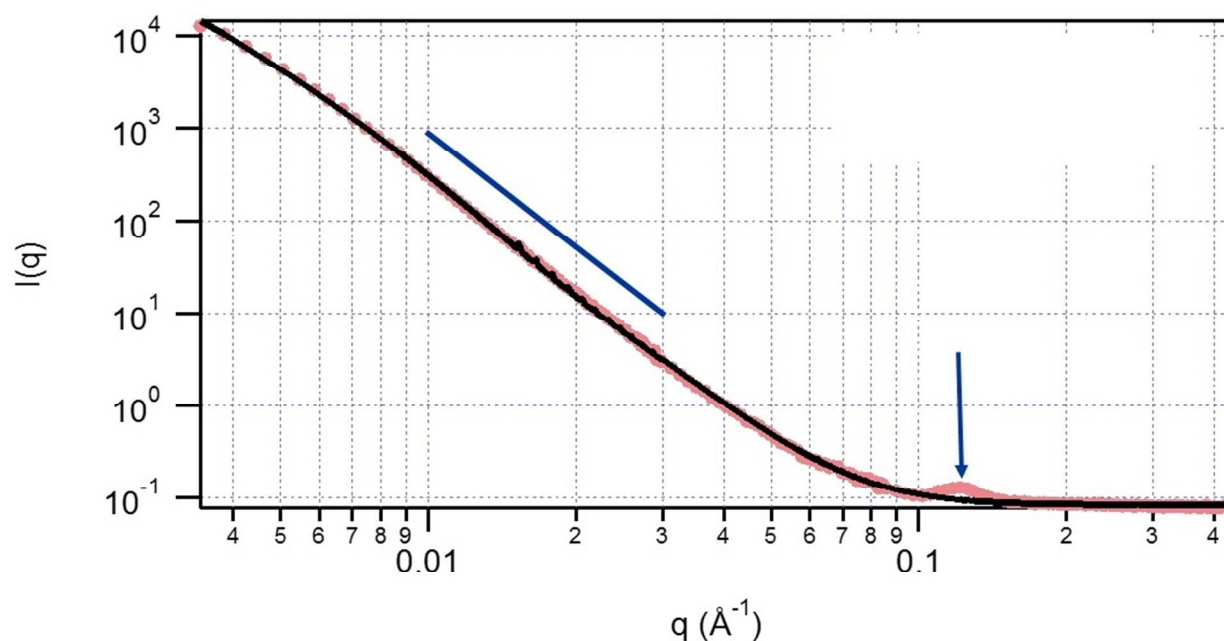


Figure 3. Log-log plot of SANS intensity (I) versus Q profile of a fast-cooled 2 wt % **HS-2-OH** in toluene- d_8 gel. (•). The black line is the theoretical curve for cylinders with poly radii: radius 28 Å, contour length 1.7×10^7 Å, Kuhn length 190 Å and polydispersity of radius 1.8. The arrow shows the second oscillation peak at $d = 52.0$ Å. The slope of the blue line is -4.

Several examples of **SAFINs** with helical structures, including **LMOGs** containing chiral alkyl chains,³⁵ sugar derivatives³⁶ triphenylbenzenes with alkoxy side chains³⁷ and cholesterol derivatives,³⁸ have been reported. Also, enantiopure **HSA** derivatives and their alkali metal salts exhibit circular dichroic signals that are attributed to helical arrangements of the molecules in their fibrillar networks.³⁹ **SAFIN** elements within the gels of 2 wt % **HS-2-OH** in silicone oil (Figure 4) and isostearyl alcohol (Figure S12A) were helical, with pitches of 130 ± 30 and 60 ± 5 nm, respectively.⁴⁰ In combination with the XRD and SANS data (both obtained in a different liquid), the AFM images of the silicone oil gel indicate that individual fibers are bundled to produce the rope-like objects of ca. 100 nm diameters (based on 10 measurements) in Figure 4. There is precedent for rope-like structures in other **SAFINs**.^{35c}

Although attempts to record AFM images of **SAFINs** of a 2 wt % **HS-2-OH** in toluene gel were unsuccessful—the liquid evaporated partially before the true gel images could be recorded—the presence of fibrillar **SAFINs** is evident (Figure S12B). An image of the corresponding xerogel showed a fibrillar structure more clearly (Figure S12C). Also, attempts to study the morphology of the **SAFIN** network of this gel using cryo-SEM were not successful, perhaps due to sample preparation protocols; the images showed a highly inhomogeneous **SAFIN** that was not consistent with the AFM and POM images.

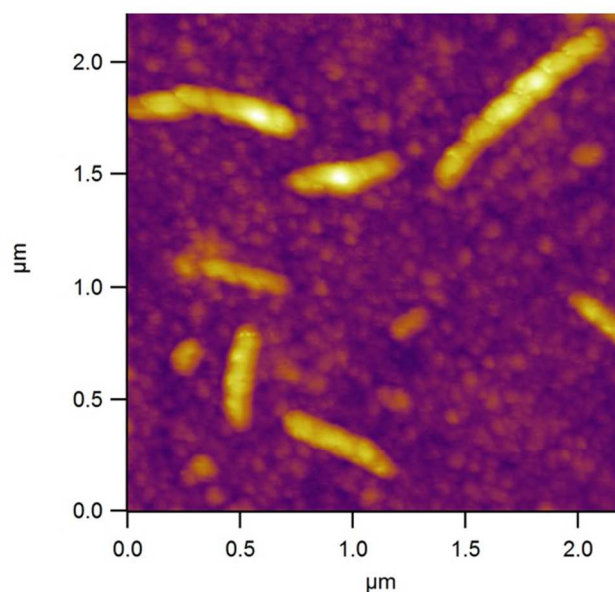


Figure 4. AFM image of a 2 wt % **HS-2-OH** in silicone oil gel.

If compared with and normalized to the heats of melting of the neat **LMOGs** (ΔH for the **LMOGs** in their gels are normalized to 100% concentrations of **LMOG** by multiplying the obtained ΔH value of the gel by $[100/((\text{total wt \% LMOG})-CGC)]$), the enthalpies (ΔH) of melting of the gels from differential scanning calorimetry (DSC) measurements can be related to the degree of crystallinity or amorphous nature of the **SAFINs**.⁴¹ Although most experiments were performed with 2 wt % of **LMOG**, DSC experiments were performed on isostearyl alcohol gels with 5 wt % **LMOG** in order to decrease errors in the calculation of ΔH values. The

normalized ΔH values for melting those gels and the heats of melting of the neat solids are very similar, and the heats of melting of the gels are similar for the four **HS-n-OH** (Table 2). Also, the T_{gel} values of the gels measured by DSC showed an odd-even effect with respect to **n**, but not when measured by the (less precise) falling drop method (Table 1). From the observation that both ΔH and $T_{gel-DSC}$ values of the **HS-3** gel are larger than those of the **S-3-OH** gel, we conclude that a larger stabilizing effect on the **SAFIN** network is realized by placing a hydroxyl group at C12 of the octadecanoyl chain than at the ω -position of the *N*-alkyl chain. However, the T_{gel} values of these gels, measured by the falling drop method, did not show an odd-even effect; all of the values are similar.

Although the number of homologues investigated is too small to derive a great deal of information from the aforementioned odd-even effect, it cannot be ascribed to different *CGC* values for the **HS-n-OH** in isostearyl alcohol gels; their similarity (Table 1) requires that nearly equal amounts of the **LMOGs** participate in each of their **SAFINs**. One possibility is that the ΔH and $T_{gel-DSC}$ differences result from conformational effects in the ω -hydroxyalkyl groups that are similar to the odd-even effects documented in liquid crystals, such as phosphatidylcholines with ω -tertiary-butyl fatty acyl chains.⁴²

Rheological studies. The yield strain of a gel consisting of 2.0 wt % **HS-2-OH** in isostearyl alcohol was < 1 % at 1 rad/s (Figure S13). At 0.05 % strain, the storage (G') and loss (G'') moduli values were independent of the applied frequency and G'/G'' remained >1 throughout ($G' \sim 2400$ Pa at $\omega = 1$ rad/s and $\gamma = 0.05$ %; Figure S14); this material is a true viscoelastic gel. A 2.0 wt % **HS-3-OH** in isostearyl alcohol gel exhibited a yield strain of < 0.1 % (Figure S15), indicating that it is mechanically weaker than the 2.0 wt % **HS-2-OH** in silicone oil gel, but both are real gels (Figure S16). The 2 wt % **S-3-OH** in isostearyl alcohol gel is

viscoelastic ($G' \sim 230$ Pa at $\gamma = 0.05$ % and $\omega = 1$ rad/s; Figure S20), but mechanically weaker than the corresponding **HS-3-OH** gel, presumably due to the absence or presence, respectively, of a hydroxyl group at C12 of the octadecanoyl chain. Based on G' values within the linear viscoelastic regions (i.e., $\gamma = 0.05$ % strain and $\omega = 1$ rad/s), the mechanical strengths of the 2 wt % **LMOG** in isostearyl alcohol gels are in the order: **HS-2-OH**>**HS-3-OH**>**S-3-OH**>**HS-4-OH**, **HS-5-OH**. The mechanical strengths of the gels with 2 wt % **HS-n-OH** in isostearyl alcohol became weaker as the ω -hydroxyalkyl chain lengths (i.e., the values of **n**) increased (Figures S13-S15 and S17-S19). Although the cause of this trend cannot be determined with the information in hand, it may be related to changes in lipophilicity, the modes of inter- and intra-molecular H-bonding involving the ω -hydroxyl group, or a combination of these factors.

Rheologically, 2 wt % of all of the **HS-n-OH** homologues in silicone oil were true gels, and altering the length of the *N*-alkyl chain did not change significantly their G' values within the linear viscoelastic regions ($G' \sim 10000$ Pa at $\gamma = 0.05$ % and $\omega = 1$ rad/s) (Figures S21-S27). They were mechanically stronger than the corresponding isostearyl alcohol gels, for which the values of G' *did* depend on the **HS-n-OH** homologue. Additional analyses of rheological data is presented below.

Kinetic studies of gel formation. Although the kinetics of nucleation and primary and secondary crystallization leading to macroscopic phase separation and gel formation have been reported previously for other **LMOG**-based systems,⁴³ the aggregation steps are usually very fast after a sol has been cooled to a temperature below the gel melting temperature (T_{gel}). Fibrillar networks of **LMOGs** consist of fractal objects that dissolve at least partially (so that the **SAFIN** is no longer intact) upon heating to above T_{gel} , and they reform at temperatures below T_{gel} . The nature of the **SAFIN** of a molecular gel can be related to the relevant nucleation and growth

kinetics by the Avrami equation (eq 1), developed originally to study the kinetics of crystallization of polymer melts and other processes involving phase ordering.⁴⁴ The Avrami exponent n (theoretically 1, 2, 3, or 4, or half-integers) is temperature independent as long as the type of the nucleation and growth mechanisms do not change.⁴⁵ The model upon which these equations is based assumes that nucleation occurs either instantaneously (zero-order) or linearly (first-order), and that the small domains of the separated phase grow independently. The meaning of the value of n is somewhat ambiguous because it depends on both crystal nucleation and growth. For this reason, the parameters obtained from the Avrami equation for gels that have similar shapes for their **SAFIN** elements and different nucleation mechanisms are not comparable.^{43c}

Fractal structures of gels with polymers and **LMOGs** have been studied as well.^{46,47} One of the most important defining parameters of a fractal object is its mass fractal dimension, D_f . It, like the Avrami n value, can provide information about the structure of a gel and the kinetics of its formation.⁴⁶ For example, Liu and coworkers^{43b,c} have studied the formation of organogels comprised of *N*-lauroyl-*L*-glutamic acid di-*n*-butylamide as the **LMOG** and isostearyl alcohol as the liquid using the Avrami equation,⁴³ and they have correlated n with D_f . We have reported that the Avrami component n from gelation of ethyl acetate by 3β -cholesteryl *N*-(2-naphthyl) carbamate changes from ~ 1 to ~ 2 at a specific incubation temperature of the sol phases.^{43b,c} Here, the aggregation and gelation processes were monitored in time primarily by changes in G' . The data were analyzed according to the Avrami equation (eq 1)⁴⁴ as well as the Dickinson equation (eq 2) that probes the fractal nature of the gels.⁴⁸ Thus, the volume fraction of a gel phase at time = t , ϕ_g^t , can be expressed in terms of G' as $\phi_g^t = \frac{G'(t) - G'(0)}{G'(\infty) - G'(0)}$, where $G'(0)$, $G'(t)$, and

$G'(\infty)$ are the values at times = 0 (i.e., before a noticeable increase in G' is observed), t , and ∞ (i.e., after a plateau value of G' has been attained), respectively. For some data sets, different $G'(0)$ and $G'(\infty)$ values were attempted to determine whether more linear fits to eqs 1 and 2 could be achieved; in some cases, small improvements were found, but the changes in the values of K and D_f were small.

In eq 1, K is a temperature-dependent parameter that is like a rate constant. In eq 2, C is a constant.

$$1 - \phi_g^t = \exp(-Kt^n) \quad (1)$$

$$\ln \phi_g^t = C + (3 - D_f) / D_f \ln t \quad (2)$$

At very early times, G' and G'' are very small, as expected of a low viscosity liquid (Figures S28-S32). Thereafter, both moduli increase, and the plateau value of G' is larger than that of G'' if gelation has occurred.⁴⁹

In 2 wt % **HS-n-OH** in isostearyl alcohol gels, a drastic decrease of gel formation time was observed: from ~40 h for **HS-2-OH** to 200 s for **HS-4-OH**, and the corresponding K values increased in the same order (Table 2). In isostearyl alcohol at 2 wt % of **LMOG**, the **S-3-OH** gel formed faster (~200 min) than that of **HS-3** (~760 min) (Table 2). Based on their storage moduli (G') values (Table 2; G'_∞ in Figures S28-S32), the mechanical strengths of the gels decreased in the reverse order of the formation times **HS-2-OH** > **HS-3-OH** > **HS-4-OH**. However, this trend was not universal—the gel formation time for **HS-5-OH**, >16 h, was longer than that of **HS-4-OH**; additional homologues should be investigated before hard conclusions are reached.

Of the 2 wt % **LMOG** in isostearyl alcohol gels, the one with **HS-3** exhibited the largest G' value, 70 kPa (Table 1). The G' value of the **S-3-OH** gel was ~ 8 times larger than that of the **HS-4-OH** or **HS-5-OH** gel and ~ 5 times smaller than that of the **HS-3-OH** gel. Thus, removing the hydroxyl group from C12 of the octadecanoyl chain (as in **S-3-OH**) weakens the **SAFIN** network. The reasons for this effect are the same as those used to explain the weaker gelating properties of stearic acid derivatives than **HSA** derivatives—the lack of a secondary H-bonding network along the octadecanoyl chains that increases their flexibility.²²

The Avrami exponents n for 2 wt % **HS-n-OH** (where $n = 2, 3$ and 4) and **S-3-OH** in isostearyl alcohol gels that were formed by fast-cooling their sols to 25 °C and incubating there (Figures S33-S36) are ~ 1 in all cases. This liquid was selected for the kinetic studies because it has a very high boiling point; it minimizes evaporation over the long periods needed to collect these rheological data.⁵⁰

An Avrami exponent of 1 indicates instantaneous, linear growth of a **SAFIN** (i.e., early nucleation followed by one-dimensional growth of the microcrystallites).⁵¹ Similarly, for all of the gels investigated, D_f values were ~ 2 (Table 2), indicating that the **LMOGs** undergo one-dimensional aggregation and growth during gelation.⁵² This conclusion is also reached by treating the data according to Avrami theory. Values of D_f between 1 and 1.5 indicate fiber-like **SAFINS**^{52a} while values between 1.5 and 2 predict spherulitic **SAFIN** structures (consisting of smaller fiber objects).⁵² The predictions about the shapes of the **SAFIN** objects from application of eqs 1 and 2 are also consistent with POM images in Figures 5 (**HS-2-OH**) and S37 (**HS-3-OH**, **HS-4-OH**, and **HS-5-OH**) for the isostearyl alcohol gels. The G' and K values of 2 wt % **HS-3-OH**, **S-3-OH**, and **HS-3** in isostearyl alcohol gels did not show a general trend: the K

value of **HS-3-OH** was ~ 40 and ~ 65 times larger than those of **S-3-OH** and **HS-3-OH**, respectively, whereas their G' values decreased in the order of **HS-3**>**HS-3-OH**>**S-3-OH**. Different factors determine the mechanical properties and the rates of aggregation leading to **SAFIN** formation.

Table 2: Thermodynamic, kinetic and thixotropic parameters related to isostearyl alcohol gel properties at 2 wt % **LMOG** (unless specified otherwise). $T_{gel-DSC}$, normalized heats (ΔH) for the **LMOGs** in their gels with ΔH of the neat **LMOG** in parentheses, approximate gel formation times from sols incubated at 25 °C ($time_{gel}$), G' values, Avrami parameters (n and K), fractal dimensions (D_f), recovery times after cessation of destructive strain (τ), and % of thixotropic recovery after cessation of destructive strain. See Supporting Information figures for data from which the various parameters were calculated.

| LMOG | Thermodynamic/Kinetic | | | | | | | Thixotropic | |
|----------------|---------------------------|------------------------|-------------------|-------------|----------------|----------------------|---------------|-----------------|---------------------------|
| | $T_{gel-DSC}, ^\circ C^a$ | $\Delta H, kJ/g^{a,b}$ | $time_{gel}, min$ | G', kPa^c | $n (R^2)^d$ | K, s^{-1}^e | $D_f (R^2)^d$ | τ, s | % of thixotropic recovery |
| HS-2-OH | 65.6 | 0.13 (0.14) | 2340 | 2.5 | 0.85 (0.97) | 8.1×10^{-6} | 2.0 (0.98) | $\sim 0.4^f$ | $>99^f$ |
| HS-3-OH | 63.9 | 0.14 (0.13) | 7 | 1.3 | 0.98 (0.98) | 1.8×10^{-3} | 2.2 (0.99) | ~ 0.6 | >99 |
| HS-4-OH | 73.2 | 0.13 (0.11) | 3 | 0.03 | 1.2 (0.97) | 9.5×10^{-3} | 1.6 (0.99) | ~ 1000 | >99 |
| HS-5-OH | 67.6 | 0.10 (0.08) | >1000 | 0.03 | - | - | - | ~ 45 | >99 |
| S-3-OH | 45.8 | 0.10 (0.08) | 200 | 0.24 | 1.1 (0.97) | 4.5×10^{-5} | 1.9 (0.96) | Not thixotropic | 0 |
| HS-3 | 68.0 | 0.17 (0.20) | 760 | 70 | 1.4 (0.99) | 2.7×10^{-5} | 1.5 (0.99) | $\sim 75^f$ | $>99^f$ |

^a 5 wt % **LMOG**. ^b ΔH for the **LMOGs** in their gels and ΔH of the neat **LMOG** in parentheses; see text for details of calculations. ^c At 1 rad/s, 0.05 % strain, 25 °C. ^d Square of the correlation coefficient for the fit. ^e One data set and fitting routine were used to obtain the R^2 values of K and n . ^f After cessation of the second application of destructive strain. See text for details.

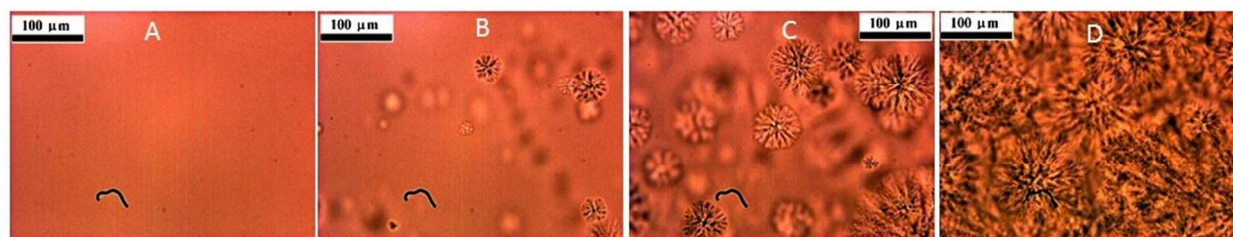


Figure 5. POM images at 25°C of a 2 wt % **HS-2-OH** in isostearyl alcohol sol at different times after being fast-cooled from 110 to 25 °C (at ~20 °C/min): (A) 0 min; (B) 7 min; (C) 15 min; (D) 110 min. The images were taken with a full-wave plate.

Thixotropic properties. A high degree of thixotropy is observed rarely in molecular gels having crystalline **SAFINS**, such as those found in the **HS-n-OH**, **S-n-OH** or **HS-3** gels. As mentioned in the Introduction, several reports have attempted to explain the thixotropic behavior of **LMOG**-based organogels with crystalline **SAFINS**.^{12,20,21,22}

Here, the thixotropic experiments are concentrated on 2 wt % gels in isostearyl alcohol; data for a 2 wt % **HS-2-OH** in silicone oil gel are included in Figure S42. More volatile liquids, such as toluene, could not be used because they evaporated somewhat during the protracted periods needed to complete the rheology experiments. However, a 2 wt % **HS-2-OH** in toluene gel was noted qualitatively to be thixotropic.

Thixotropic experiments were conducted with a 2 wt % **HS-3-OH** in isostearyl alcohol gel at 25 °C under initial conditions at which the gel is stable (a strain of 0.05 % and angular frequency of 100 rad/s) for 150 s to establish baseline values for G' and G'' . Figure S43 shows the evolution of G' and G'' after applying a 30 % strain to the gel, conditions that lead to loss of its gel properties. Then, the original conditions were re-applied in order to monitor the recovery of the viscoelasticity: *~99 % of the original G' value was recovered, and the experiment was reproduced over several cycles* (Figures 6 and S44).

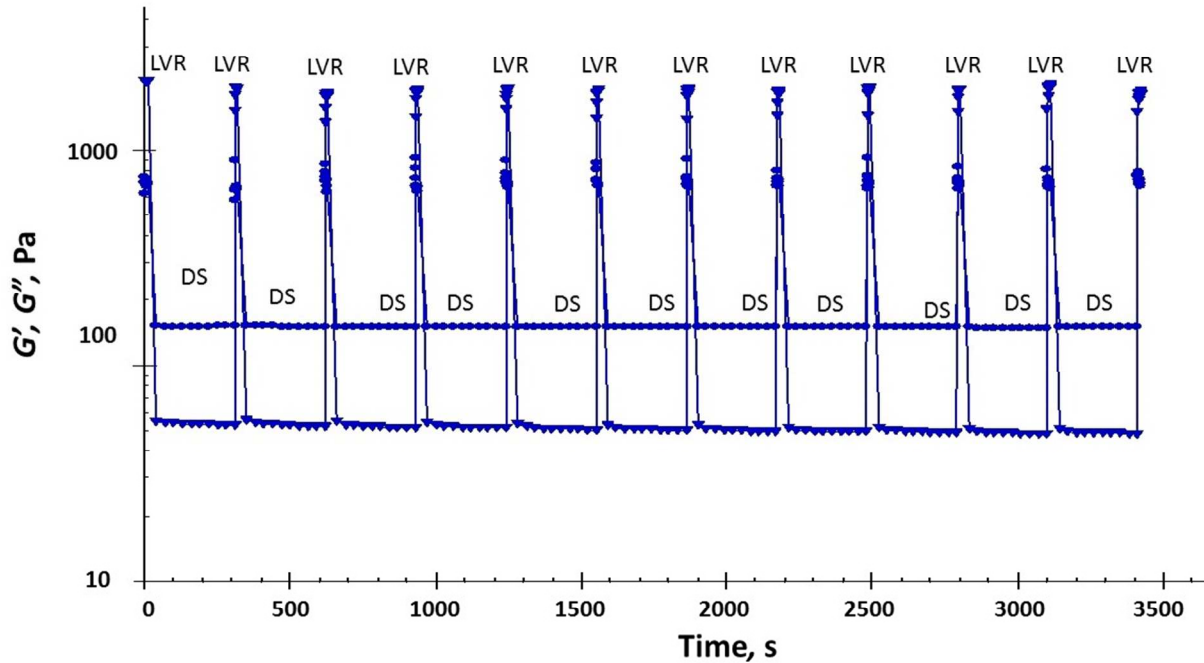


Figure 6. G' (\blacktriangledown) and G'' (\blacksquare) at 25 °C as a function of time and application of different strains and frequencies to a fast-cooled 2.0 wt % **HS-3-OH** in isostearyl alcohol gel. Linear viscoelastic region (LVR): $\gamma = 0.05$ %, $\omega = 100$ rad/s. Destructive strain (DS): $\gamma = 30$ %, $\omega = 1$ rad/s. Rotational strain was kept at 0 % for 0.05 s before changing from DS to LVR conditions.

To investigate the nature of the thixotropy, the rheological data were analyzed using a stretched exponential model (eq 3)⁵³ in which τ is a time constant representing the recovery speed and m is a dimensionless constant. This equation is similar to the Avrami equation when it is in a logarithmic form. As mentioned regarding the data treatments associated with eqs 1 and 2, fits with some variation of the $G'(0)$ and $G'(\infty)$ values were examined, and the resulting changes in τ were small.

$$\ln\left[-\ln\frac{G'(\infty)-G'(t)}{G'(\infty)-G'(0)}\right]=m\ln t-m\ln\tau \quad (3)$$

Figure S45 shows the recovery of G' after applying and then removing a destructive strain to a 2 wt% **HS-3-OH** in isostearyl alcohol gel for ten consecutive runs (Figure 6). From

the average of the G' values for the ten consecutive cycles (Figure S46) and eq 3, τ was calculated to be very fast, ~ 0.6 s.

Figure S47 shows the evolution of G' and G'' after applying a 30 % (destructive) strain to a **HS-2-OH** in isostearyl alcohol gel. When the original non-destructive conditions (0.05 % strain and 100 rad/s angular frequency) were applied, only 38 % of the original G' value was recovered: G' decreased from 13000 to 5300 Pa, and G'' decreased from 1600 to 700 Pa. However, subsequent destruction-recovery cycles resulted in > 99 % recovery of the storage modulus ($G' = 5300$ Pa) (Figure S48). From these data, τ was calculated to be even faster than for the **HS-3-OH** gel, ~ 0.4 s (Figure S49)!

Similar rheological experiments were conducted with 2 wt % **HS-4-OH** and **HS-5-OH** in isostearyl alcohol gels at 25 °C: first, for 150 s under conditions at which the gel is stable (0.05 % strain and 1 rad/s angular frequency), followed by application of a destructive (30 %) strain. Figures S50 and S51 show the temporal evolutions of G' and G'' after re-applying the initial conditions (where the gel is stable). Again, the eventual recoveries of G' were ~ 99 %, and the values of τ were ~ 1000 and ~ 150 s for the gels of **HS-4-OH** (Figure S52) and **HS-5-OH** (Figure S53), respectively. Note that the addition or subtraction of one methylene unit, the differences among **HS-3-OH** and **HS-4-OH** and **HS-5-OH**, had no discernible effect on the eventual recovery of viscoelasticity (nearly complete for the 3 homologues), but it caused a nearly 1000 fold change in the *rate* of recovery! A possible explanation for the different recovery times may be related to the G' values and mechanical strengths of the gels. The strength of the **HS-4-OH** gel is less than that a **HS-3-OH** or **HS-2-OH** gel (Figures S22, S23, and S26). The gel formation times are in the order: **HS-2-OH** < **HS-3-OH** < **HS-4-OH**. Except for 2 wt % **HS-5-OH** in the isostearyl alcohol gel, τ values of the mechanically stronger gels (i.e., having larger G' values)

are shorter than those of the weaker gels. The τ value of the **HS-5-OH** gel is ca. 20 times longer than that of the **HS-4-OH** gel while the storage moduli of both gels are ~ 30 Pa. We speculate that stabilization by secondary H-bonding interactions in **SAFINs** of **LMOGs** having a C12 hydroxyl group may also influence the strengths of junction zones and, thus, both the strain needed to destroy a gel and the ease with which it can reform after the cessation of destructive strain. Because we lack detailed information about the molecular interactions at junction zones, it is not possible to state whether the lower *CGCs*, the shorter gelation times from sols incubated at 25 °C, and the higher mechanical strengths are indicators of higher or lower τ values; see Table 2. However, based on qualitative entropic considerations, one might have argued (incorrectly!) that weak gels should be less discriminating than strong gels in their reassembly after cessation of destructive strain (i.e., recover more rapidly) and should exhibit higher degrees of recovery.⁵⁴

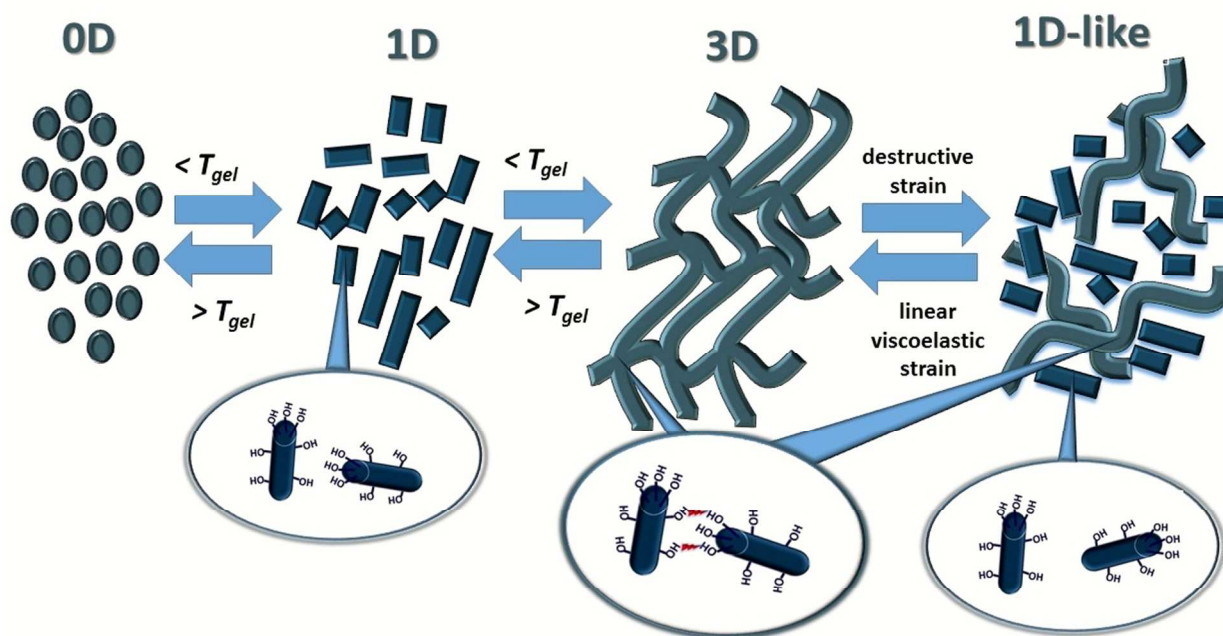
Figure S54 shows the evolution of G' and G'' after cessation of the application of a 30 % (destructive) strain to the 2 wt % **HS-3** in isostearyl alcohol gel. Only ~ 65 % of the original G' value, 67000 Pa, was recovered. However, ca. 99 % of the 43600 Pa storage modulus was found after the first recovery cycle (Figure S55). From the average of the G' values (Figure S56) and eq 3, τ was calculated to be about ~ 75 s. Unlike the isostearyl alcohol gels with **HS-n-OH** and **HS-3** (Figures S54-S56), a 2 wt % **S-3-OH** in isostearyl alcohol gel did not recover its viscoelasticity after applying destructive strain (Figure S57). However, *N*-3-hydroxypropyl dodecanamide in toluene gels do exhibit thixotropic properties.²⁰ Note also that **S-3-OH** did not gelate toluene. Destruction of the *N*-3-hydroxypropyl dodecanamide in toluene gel was ascribed to the fibers of the **SAFIN** becoming disconnected and aligned in the sol phase.²⁰ The reasons why *N*-3-hydroxypropyl dodecanamide is able to gelate toluene and why those gels are

thixotropic may be related to the same factors that are responsible for the **HS-n-OH** in isostearyl alcohol gels being thixotropic. In isostearyl alcohol at 2 wt % of the **LMOG**, thixotropic recovery of the **HS-3** gel is ~125 times slower than that of the **HS-3-OH** gel even though the G' value of former is ~50 times larger. Clearly, these differences must be related to the respective H-bonding networks within the **SAFINs** and in the sol phases produced by the destructive strain.

Also, although the Avrami K values decreased as the gelation times, $time_{gel}$, increased, (Figure S58), no correlation was apparent between either K or $time_{gel}$ and τ , the time for gel recovery after cessation of destructive strain. That lack of correlation indicates that somewhat different processes are responsible for molecular aggregation and nucleation leading to **SAFINs** and reestablishment of the **SAFINs** from their fibrillar components even when the reformed gel and the one before application of destructive strain have the same mechanical properties. Whereas both K and $time_{gel}$ monitor aggregation and nucleation of the '0-dimensional' (0D) **LMOGs**, and their growth into '1-dimensional' (1D) fibers and finally into the '3-dimensional' (3D) **SAFINs**, the processes associated with τ start with 1-dimensional objects and follow their reassembly into 3-dimensional ones. Thus, the reassembly times in the thixotropic measurements are not directly related to the parameters that follow aggregation starting from single **LMOG** molecules.

What is the source of thixotropy in **HS-n-OH**-based gels? As shown in Scheme 1, when the 0D objects, representative of the **HS-n-OH** molecules in sols or solutions, are cooled below T_{gel} , they aggregate into 1D fibers that are joined at "junction zones" to form 3D **SAFINs** and immobilize the liquid.⁷ The data provided in the text indicate that the **SAFINs** of the gels are stabilized by intermolecular H-bonding interactions involving the C12 hydroxyl groups of the octadecanoyl chains, the terminal ω -hydroxyl moieties on the *N*-alkyl chains, and the amide

groups. According to this model, upon application of destructive strain, the H-bonding interactions among the ω -hydroxyl groups at or near junction zones (Scheme 1) are weakened, broken or disrupted preferentially, without disassembling the individual fibers. Disassembly of the **SAFINs** in this way would lead to macroscopic fluidity of the sample while reassembly would depend on the ability to re-establish inter-fiber ω -hydroxyl H-bonding networks. Given the very short times needed for sols of **HS-2-OH** and **HS-3-OH** to reform after the cessation of destructive strain, there must be very little selectivity in the positions on fiber surfaces where they can rejoin. A reasonable hypothesis is that many hydroxyl groups lie along the surfaces of the fibers.



Scheme 1. Cartoon representations of a possible mechanism for thermal and mechanotropic destruction and reformation of **SAFINs** in **HS-n-OH** gels.

We conjecture that the **HS-n-OH** **SAFINs** in the isostearyl alcohol gels are held together by hydroxyl groups at junction zones (i.e., the weak points where fibers intersect),²⁰ and that they interact with the amide functionalities to form internal H-bonding networks within the fibers. In

a fashion similar to the way that the -OH groups of phosphonium salts are able to solvate specifically the cationic and anionic parts of their ‘head groups’,²³ the ω -hydroxyl groups of the **HS-n-OH** can ‘lubricate’ intermolecular interactions within the fibers of the **SAFINs**. When destructive strain is applied, the junction zones are cleaved and the gel phase becomes a sol. If the junction zones in the **HS-n-OH**-based gels consist (in large part) of ω -hydroxyl groups on the *N*-alkyl chains and many hydroxyl groups lie along the lateral surfaces of the fibers, the **SAFINs** can be reestablished easily when destructive strain ceases. In this scenario, the rate of recovery will depend on the rates of diffusion of the fibers and entropic requirements for inter-fiber interactions that depend on the specific packing within the **SAFINs** made by each **LMOG**.

However, other factors must be at play even if the ‘lubrication’ model described here is correct. It is known that silicone oil gels of (*R*)-12-hydroxystearamide, an **LMOG** that has no ω -hydroxyl ‘lubricating group’, are able to recover ~90 % of their original viscoelasticity within 10 s after the cessation of destructive strain.²² The corresponding silicone oil gels of the secondary amides, (*R*)-12-hydroxy-*N*-alkyloctadecanamides, recover only about one-half of their initial G' value after cessation of destructive strain, and those with **LMOGs** that are amine derivatives of **HSA** recover less than 10 % of their initial G' values.²² Within this series of **LMOGs**, the degree of recovery can be qualitatively correlated with the potential strength of hydrogen-bonding interactions among the **LMOGs**.²²

Conclusions.

Several correlations between structural aspects of the **LMOGs** examined here and the properties of their **SAFINs** and gels have been found. XRD and POM studies indicate that the **SAFIN** networks of the **HS-n-OH** gels are crystalline. However, although XRD diffractograms of neat **HS-n-OH** gelators have been satisfactorily indexed as orthorhombic, all of the **SAFINs**

of the isostearyl alcohol gels except that of **HS-2-OH**, exhibit different morphologies than their neat solids that could not be indexed.

As reported previously with other derivatives of **HSA** and stearic acid,²² the *CGC* values of the gels with **HS-3-OH**, an **LMOG** with a hydroxyl group at C12 of the octadecanoyl chain, are lower than that those of the gels with **S-3-OH**, the analogous **LMOG** lacking a hydroxyl group at C12. The presence of the hydroxyl group results in the formation of a secondary H-bonding network along the long alkyl chains that is able to aid the stabilization of the **SAFINs** through enhanced intermolecular interactions of octadecanoyl chains. For example, the *CGC* of the **HS-3-OH** in silicone oil gel, 0.08 wt %, is exceptionally low and is significantly lower than that of the corresponding **S-3-OH** gel (as well as that that of **HS-3**, the **LMOG** with a C12 hydroxyl group but lacking a ω -hydroxyl group on the *N*-alkyl group). Similarly, at 2 wt %, the T_{gel} values of the silicone oil gels correlate with the amounts of each of these **LMOGs** within their **SAFINs**: that of **HS-3-OH** is the highest and that of **S3-OH** is the lowest. Although the *CGC* values were similar for all of the homologues of the **HS-n-OH** in several liquids, the mechanical strengths became weaker with increasing *n*. Comparisons of the *CGCs* of the gels in other liquids, especially those of higher polarity, do not lead to as clear conclusions.

In principle, T_{gel} values should depend on the melting temperature of the neat gelator, the method used to prepare the gel, the properties of the liquid component, and, as noted above, the *CGC* values. For example, both the melting points of the neat **HS-n-OH** and the T_{gel} values of their silicone oil gels decrease as *n* increases. Also, the melting temperature of **S3-OH** was lower than those of **HS-3-OH** and **HS-3**, both of which do have a hydroxyl group at C12. The same trend was found in the T_{gel} values and mechanical strengths of their 2 wt % gels in isostearyl alcohol; silicone oil and toluene gels, for which other comparisons were possible, showed the same trends between gelator structure and T_{gel} .⁵⁵

The Avrami exponents (~ 1) and fractal dimensions (~ 2), found for all of the isostearyl alcohol gels (including those of **HS-3** and **S-3-OH**), suggest spontaneous, linear growth of **SAFIN** fibers in bundles. Consistent with these parameters, the POM images show spherulites, and an AFM image of a silicone oil gel revealed fibrous bundles shaped like twisted ropes. Also, while the Avrami K values decreased as the gelation times, $time_{gel}$, increased, (Figure S57), no correlation was apparent between either K or $time_{gel}$ and τ , the time for gel recovery after cessation of destructive strain.

Although the model advanced to explain the static and dynamic natures of the **HS-n-OH** gels examined here will require additional testing and refinement, it seems to encapsulate the basic factors that control thixotropy in this class of gels. It and the observations that (1) very high degrees of thixotropy are possible in gels with crystalline **SAFINs** comprised of **LMOGs** and that (2) the recovery times for sols produced by mechanical destruction of the gels can be modulated on the basis of specific H-bonding interactions and minor structural changes constitute some of the most important new scientific insights reported here. As mentioned, formation of gels from sols by cooling or by the cessation of destructive strain involve different processes. In the former, 0D objects assemble to 1D species before becoming 3D **SAFINs**. In the latter, the initial stage involves 1D or even pieces of a **SAFIN** (such as non-interacting spherulites). These differences are responsible for the lack of correlation noted above between the rates of gel formation from incubated sols and from mechanically destroyed gels. Understanding the bases for the dynamics of gel formation by different routes, as has been explored here, should aid in the design of other thixotropic materials. In that regard, the concepts presented here will be extended to other systems in future studies.

Acknowledgments. We thank the National Science Foundation (Grant CHE-1147353) and the Gulf of Mexico Research Initiative for their support of this research. Prof. Dganit Danino at the Technion, Dr. Sophia Hohlbauch and Mr. Rob Cain of Bruker Corporation and Dr. Xinran Zhang of the Institute for Soft Matter Synthesis and Metrology at Georgetown are thanked for helpful discussions and assistance in obtaining data. We are grateful to Drs. Paul Butler and Katherine Weigandt of the Center for Neutron Research at the National Institute of Standards and Technology for help with the SANS experiments. We acknowledge the support of the National Institute of Standards and Technology, U.S. Department of Commerce, in providing the neutron research facilities used in this work.

Supporting Information. Experimental details and procedures, XRD and SANS diffractograms, POM and AFM images, strain and frequency sweep rheology curves, kinetic plots of gel formation, and thixotropic plots of gel destruction and recovery. This material is available free of charge via the Internet at <http://pubs.acs.org>.

References

¹ a) X. He, M. Aizenberg, O. Kuksenok, L. D. Zarzar, A. Shastri, A. C. Balazs and J. Aizenberg, *Nature*, 2012, **487**, 2014-2018. b) A. Llordes, G. Garcia, J. Gazquez and D. J. Milliron, *Nature*, 2013, **500**, 323-328. c) J. Liua, C. Xiea, X. Daia, L. Jinb, W. Zhoua and C. M. Liebera, *Proc. Natl. Acad. Sci. USA*, 2013, **110**, 6694-6699.

² a) J.-L. Pozzo, G. M. Clavier and J.-P. Desvergne, *J. Mater. Chem.*, 1998, **8**, 2575-2577. b) S-i Tamaru, M. Nakamura, M. Takeuchi and S. Shinkai, *Org. Lett.*, 2001, **3**, 3631-3634. c) G. Mieden-Gundert, L. Klein, M. Fischer, F. Vögtle, K. Heuzé, J.-L. Pozzo, M. Vallier and F. Fages, *Angew. Chem., Int. Ed.*, 2001, **40**, 3164-3166.

-
- ³ S. Shinkai and K. Murata, *J. Mater. Chem.*, 1998, **8**, 485-495.
- ⁴ J. H. van Esch, and B. L. Feringa, *Angew. Chem. Int. Ed.*, 2000, **39**, 2263-2266.
- ⁵ N. M. Sangeetha and U. Maitra, *Chem. Soc. Rev.*, 2005, **34**, 821–836.
- ⁶ R. G. Weiss and P. Terech, *Molecular Gels. Materials with Self-Assembled Fibrillar Networks*, Springer, Netherlands, 2006.
- ⁷ P. Terech and R. G. Weiss, *Chem. Rev.*, 1997, **97**, 3133-3159.
- ⁸ M. George and R. G. Weiss, *Acc. Chem. Res.*, 2006, **39**, 489-497.
- ⁹ R. Shankar, T. K. Ghosh and R. J. Spontak, *Soft Matter*, 2007, **3**, 1116-1129.
- ¹⁰ W. Edwards, C. A. Lagadec and D. K. Smith, *Soft Matter*, 2011, **7**, 110-117.
- ¹¹ A. Dawn, T. Shiraki, S. Haraguchi, S.-i. Tamaru and S. Shinkai, *Chem. Asian J.*, 2011, **6**, 266 – 282.
- ¹² a) J. Brinksma, B. L. Feringa, R. M. Kellog, R. Vreeker and J. van Esch, *Langmuir*, 2000, **16**, 9249-9255. (b) X. Huang, S. R. Raghavan, P. Terech and R. G. Weiss, *J. Am. Chem. Soc.*, 2006, **128**, 15341-15352. (c) M. Shirakawa, N. Fujita and S. Shinkai, *J. Am. Chem. Soc.*, 2005, **127**, 4164-4165. (d) V. Percec, M. Peterca, M. E. Yurchenko, J. G. Rudick and P. A. Heiney, *Chem. Eur. J.*, 2008, **14**, 909-918. (e) S. Roy, A. Baral and A. Banerjee, *Chem. Eur. J.*, 2013, **19**, 14950 – 14957. f) S. K. Mandal, S. Brahmachari and P. K. Das, *Chem. Plus Chem.*, 2014, **79**, 1733 – 1746.
- ¹³ a) R. G. Weiss, *J. Am. Chem. Soc.*, 2014, **136**, 7519-7530. b) V. A. Mallia and R. G. Weiss, *J. Phys. Org. Chem.*, 2013, **27**, 310-315.
- ¹⁴ W. H. Bauer and E. A. Collins, in *Rheology: Theory and Application*, ed. F. R. Eirich, Academic Press, New York, 1967, chapter 8.
- ¹⁵ P. G. Waser, *Science*, 1957, **125**, 739.

-
- ¹⁶ C. Du, G. Falini, S. Fermani, C. Abbott and J. Moradian-Oldak, *Science*, 2005, **307**, 1450-1454.
- ¹⁷ S. Bhattacharjee and S. Bhattacharya, *Chem. Commun.*, 2014, **50**, 11690-11693.
- ¹⁸ a) S. Roy, A. K. Katiyar, S. P. Mondal, S. K. Ray and K. Biradha, *ACS Appl. Mater. Interfaces*, 2014, **6**, 11493–11501. b) T. Witte, B. Decker, J. Mattay and K. Huber, *J. Am. Chem. Soc.*, 2004, **126**, 9276-9282. c) W. Weng, J. B. Beck, A. M. Jamieson and S. J. Rowan, *J. Am. Chem. Soc.*, 2006, **128**, 11663-11672.
- ¹⁹ A. P. Sivadas, N. S. S. Kumar, D. D. Prabhu, S. Varghese, S. K. Prasad, D. S. S. Rao and S. Das, *J. Am. Chem. Soc.*, 2014, **136**, 5416–5423.
- ²⁰ M. Lescanne, P. Grondin, A. D'Aleo, F. Fages, J.-L. Pozzo, O. M. Monval, P. Reinheimer and A. Collin, *Langmuir*, 2004, **20**, 3032-3041.
- ²¹ a) S. Basak, J. Nanda and A. Banerjee, *Chem. Commun.*, 2014, **50**, 2356—2359. b) J. Nanda, S. Basak, A. Banerjee, *Soft Matter*, 2013, **9**, 4198–4208. c) X. Yu, L. Chen, M. Zhanga, T. Yi, *Chem. Soc. Rev.*, 2014, **43**, 5346-5371.
- ²² V. A. Mallia, M. George, D. L. Blair and R. G. Weiss, *Langmuir*, 2009, **25**, 8615-8625.
- ²³ a) K. Ma, B. S. Somashekhar, N. G. Gowda, C. L. Khetrapal and R. G. Weiss, *Langmuir*, 2008, **24**, 2746-2758. b) K. Ma, A. Shahkhatuni, B. S. Somashekhar, G. A. Nagana Gowda, Y. Tong, C. L. Khetrapal and R. G. Weiss, *Langmuir*, 2008, **24**, 9843-9854. c) K. Ma, L. Minkova, K.-M. Lee and R. G. Weiss, *J. Org. Chem.*, 2009, **74**, 2088-2098.
- ²⁴ A. Takahashi, M. Sakai and T. Kato, *Polym. J.*, 1980, **12**, 335-341.
- ²⁵ More detailed investigations of mixed solvent gelation by the **HS-n-OH**, as well as hydrogelation properties of **S-3-OH**, will be the topics of future studies.
- ²⁶ B.-M. Lundén, *Acta Cryst.*, 1976, **B32**, 3149-3153.

-
- ²⁷ Using Chem 3 D Ultra 8 software (Cambridge Soft Corporation, USA) and adding the van der Waals radii of the terminal atoms according to: (a) A. Bondi, *J. Phys. Chem.*, 1964, **68**, 441-451. (b) M. Mantina, A. C. Chamberlin, R. Valero, C. J. Cramer and D. G. Truhlar, *J. Phys. Chem. A*, 2009, **113**, 5806-5812.
- ²⁸ B. Dahlen, I. Pascher and S. Sundell, *Acta Chem. Scand. A*, 1977, **31**, 313-320.
- ²⁹ Drawn by adding the required atoms and bonds to single-crystal XRD structures of **HSA** methyl ester or *N*-(2-hydroxyethyl)octadecanamide using Mercury CSD 3.3 software.^a Then, the geometry was optimized using PM7 in MOPAC2012.^b a) C. F. Macrae, P. R. Edgington, P. McCabe, E. Pidcock, G. P. Shields, R. Taylor, M. Towler and J. V. D. Streek, *J. Appl. Cryst.* 2006, **39**, 453-457. b) J. J. P. Stewart, *J. Comp. Chem.*, 1989, **10**, 209-220.
- ³⁰ E. Ostuni, P. Kamaras, and R. G. Weiss, *Angew. Chem. Int. Ed.*, 1996, **35**, 1324-1326.
- ³¹ a) V. A. Mallia, P. D. Butler, B. Sarkar, K. T. Holman and R. G. Weiss, *J. Am. Chem. Soc.*, 2011, **133**, 15045–15054. b) S. Wu, J. Gao, T. J. Emgeb and M. A. Rogers, *Soft Matter*, 2013, **9**, 5942–5950. c) S. Wu, J. Gao, T. J. Emgeb and M. A. Rogers, *Cryst. Growth Design*, 2013, **13**, 1360–1366. d) G. C. Kuang, M. J. Teng, X. R. Jia, E. Q. Chen and Y. Wei, *Chem. Asian J.*, 2011, **6**, 1163-1170. e) Y. Jeong, K. Hanabusa, H. Masunaga, I. Akiba, K. Miyoshi, S. Sakurai and K. Sakurai, *Langmuir*, 2005, **21**, 586-594. f) M. H. Nielsen, S. Aloni and J. J. D. Yoreo, *Science*, 2014, **345**, 1158-1162.
- ³² a) J. S. Higgins and H. C. Benoît, *Polymers and neutron scattering*, Clarendon Press, Oxford, 1994, pp 165-174. b) P. W. A. Schmidt, *Makromol. Chem. Makromol. Symp.*, 1988, **15**, 153-166. c) M. George, S. L. Snyder, P. Terech and R. G. Weiss, *Langmuir*, 2005, **21**, 9970-9977.

³³ When the contour length was changed to 1.1×10^4 Å, the radius became 28.5 Å and the Kuhn length changed from 200 to 190 Å (Figure S7B). However, changing the Kuhn length to 900 Å and allowing the contour length and radius to vary resulted in calculated values of $\sim 10^7$ Å and 28 Å, respectively, but the match between the calculated and experimental SANS curves was very poor (Figure S7C). As such, the contour length will not be discussed here, other than to note that it is very long, and the Kuhn length is less important to us in this study than the radius. Another model examined, for parallelepiped cross-sections, did not give good fits, either (Figure S7A).

³⁴ a) J. F. Douglas, *Langmuir*, 2010, **25**, 8386-8391. b) M. A. Rogers and G. Alejandro, *Langmuir*, 2009, **25**, 8556-8566. c) R. Y. Wang, X.-Y. Liu, J. Y. Xiong and J. L. Li, *J. Phys. Chem. B*, 2006, **110**, 7275-7280.

³⁵ a) L. Brunsveld, H. Zhang, M. Glasbeek, J. A. J. M. Vekemans and E. W. Meijer, *J. Am. Chem. Soc.*, 2000, **122**, 6175–6182. b) M. A. J. Gillissen, M. M. E. Koenigs, J. J. H. Spiering, J. A. J. M. Vekemans, A. R. A. Palmans, I. K. V. Voets and E. W. Meijer, *J. Am. Chem. Soc.*, 2014, **136**, 336–343. c) S. J. George, A. Ajayaghosh, P. Jonkheijin, A. P. H. J. Schenning, E. W. Meijer, *Angew. Chem. Int. Ed.*, 2004, **43**, 3422–3425.

³⁶ a) I. Nakazawa, M. Masuda, Y. Okada, T. Hanada, K. Yase, M. Asai and T. Shimizu, *Langmuir*, 1999, **15**, 4757–4764. b) G. John, Y. Masuda, K. Okada, T. Yase, and T. Shimizu, *Adv. Mater.* 2001, **13**, 715–718. c) G. John, J. H. Jung, H. Minamikawa, K. Yoshida and T. Shimizu, *Chem. Eur. J.*, 2002, **8**, 5494–5500. d) S. Tamaru, S. Uchino, M. Takeuchi, M. Ikeda, T. Hatano and S. Shinkai, *Tetrahedron Lett.*, 2002, **43**, 3751–3755.

³⁷ C. Bao, R. Lu, M. Jin, P. Xue, C. Tan, T. Xu, G. Liu and Y. Zhao, *Chem. Eur. J.*, 2006, **12**, 3287–3294.

-
- ³⁸ (a) P. C. Xue, R. Lu, D. M. Li, M. Jin, C. H. Tan, C. Y. Bao, Z. M. Wang and Y. Y. Zhao, *Y. Langmuir*, 2004, **20**, 11234-11239. (b) J. H. Jung, S. Shinkai and T. Shimizu, *Chem. Mater.*, 2003, **15**, 2141–2145.
- ³⁹ (a) T. Tachibana, T. Mori and K. Hori, *Bull. Chem. Soc. Jpn.*, 1980, **53**, 1714-1719.
- ⁴⁰ Gels of **HS-2-OH** in silicone oil and isostearyl alcohol were not studied by SANS due to the unavailability of deuterated liquids and gelator.
- ⁴¹ P. Gill, T. T. Moghadam and B. Ranjbar, *J. Biomol. Tech.*, 2010, **21**, 167–193.
- ⁴² R. N. A. Lewis, H. H. Mantsch and R. N. McElhaney, *Biophys. J.*, 1989, **56**, 183-193.
- ⁴³ a) X.-Y. Liu and P. D. Sawant, *Appl. Phys. Lett.*, 2001, **79**, 3518-3520. b) X. Huang, P. Terech, S. R. Raghavan and R. G. Weiss, *J. Am. Chem. Soc.*, 2005, **127**, 4336-4344. c) X. Huang, P. Terech, S. R. Raghavan and R. G. Weiss, *J. Am. Chem. Soc.*, 2006, **128**, 15431-15352.
- ⁴⁴ a) M. Avrami, *J. Chem. Phys.*, 1939, **7**, 1103-1112. b) M. Avrami, *J. Chem. Phys.*, 1940, **8**, 212-224.
- ⁴⁵ a) J. M. Schultz, *Polymer Materials Science*, Prentice Hall, Englewood Cliffs, New Jersey, 1974, p 385. b) B. Wunderlich, *Macromolecular Physics*, Academic Press, New York, 1976, Vol 2, pp 16-52.
- ⁴⁶ a) T. Nakayama and K. Yakubo, *Fractal Concepts in Condensed Matter Physics*, Springer, Berlin, 2003. b) W. G. Rothschild, *Fractals in Chemistry*, John Wiley & Sons, New York, 1998. c) T. G. Deway, *Fractals in Molecular Biophysics*, Oxford University Press, New York, 1997.
- ⁴⁷ For some pertinent references, see: a) P. G. de Gennes, *Scaling Concepts in Polymer Physics*, Cornell University Press, Ithaca, 1979. b) D. Stauffer, A. Coniglio and M. Adam, *Adv. Polym. Sci.*, 1979, **44**, 103-158. c) E. Hendricks, M. Ernst and R. Ziff, *J. Stat. Phys.*, 1983, **31**, 519-563. d) P. Meakin, *Phys. Rev. Lett.*, 1983, **51**, 1119-1122. e) M. Kolb, R. Botet and R. Jullien, *Phys.*

Rev. Lett., 1983, **51**, 1123-1126. f) R. Jullien and A. Hasmy, *Phys. Rev. Lett.*, 1995, **74**, 4003-4006. g) A. Coniglio, H. E. Stanley and W. Klein, *Phys. Rev. B*, 1982, **25**, 6805-6821. h) F. Tanaka and A. Matsuyama, *Phys. Rev. Lett.*, 1989, **62**, 2759-2762.

⁴⁸ E. Dickinson, *J. Chem. Soc., Faraday Trans.*, 1997, **93**, 111-114.

⁴⁹ F. Lortie, S. Boileau, L. Bouteiller, C. Chassenieux, B. Demé, G. Ducouret, M. Jalabert, F. Lauprêtre and P. Terech, *Langmuir*, 2002, **18**, 7218-7222.

⁵⁰ Even with isostearyl alcohol as the liquid, kinetic studies of gel formation with **HS-5-OH** were not possible because the very long periods needed for gel formation. (Figure S31). Those times make the integrity of the “infinite time” values questionable.

⁵¹ R. S. H. Lam and M. A. Rogers, *Cryst. Eng. Comm.*, 2011, **13**, 866–875.

⁵² a) L. L. Hench and J. K. West, *Chem. Rev.*, 1990, **90**, 33-72. b) C. J. Brinker and G. W. Scherer, *Sol-gel science*, Academic Press, San Diego, 1989.

⁵³ H. A. Barnes, *J. Non-Newtonian Fluid Mech.*, 1997, **70**, 1-33.

⁵⁴ I. Steg and D. Katz, *J. Appl. Polym. Sci.*, 1965, **9**, 3177-3193.

⁵⁵ T_{gel} comparisons are difficult in liquids with lower boiling points, such as CCl_4 . The liquids begin to evaporate while the **SAFINs** are melting.